In vitro detection of canine anti-human antibodies following intratumoral injection of the hu14.18-IL2 immunocytokine in spontaneous canine melanoma

Short title: Analysis of canine anti-human antibodies

Andrew T. Kosharek[1¶], Cindy L. Zuleger[2,3¶], William S. Glass[4], Jens Eickhoff [3,5], Paul M. Sondel[3,6,7], David M. Vail[3,8], Mark R. Albertini[2,3,9,10*]

[1]University of Wisconsin School of Medicine and Public Health, Madison, WI, United States of America

[2]University of Wisconsin School of Medicine and Public Health, Department of Medicine, Madison, WI, United States of America

[3]University of Wisconsin Carbone Cancer Center, Madison, WI, United States of America

[4]University of Wisconsin-Madison, Madison, WI, United States of America

[5]University of Wisconsin School of Medicine and Public Health, Department of Biostatistics & Medical Informatics, Madison, WI, United States of America

[6]University of Wisconsin School of Medicine and Public Health, Department of Human Oncology, Madison, WI, United States of America

[7]University of Wisconsin School of Medicine and Public Health, Department of Pediatrics, Madison, WI, United States of America

[8]University of Wisconsin School of Veterinary Medicine, Department of Medical Sciences, Madison, WI, United States of America

[9]University of Wisconsin School of Medicine and Public Health, Department of Dermatology, Madison, WI, United States of America

[10]The Medical Service, William S. Middleton Memorial Veterans Hospital, Madison, Wisconsin, United States of America

* Corresponding author

E-mail: mralbert@wisc.edu (MRA)

¶These authors contributed equally to this work.

Abstract

Background: Canine and human malignant melanoma are naturally occurring cancers with many similarities, making the dog an important parallel patient population to study both diseases. However, development of canine anti-human antibodies (CAHA) needs to be considered when evaluating humanized biotherapeutics in dogs.

Objectives: Characterize CAHA in sera from dogs with spontaneous melanoma receiving radiotherapy and intratumoral immunocytokine (IT-IC) with humanized 14.18-IL2.

Methods: Serum samples were obtained pre-treatment and at several post-treatment times from 12 dogs with locally advanced or metastatic melanoma treated with radiotherapy to the primary site and regional lymph nodes (when clinically involved) followed by IT-IC of humanized 14.18-IL2. Two CAHA assays were developed. A sandwich enzyme-linked immunosorbent assay (ELISA) was developed to detect antibodies against the humanized IgG component of hu14.18-IL2. A flow cytometry assay was developed to determine the ability of CAHA to inhibit binding of a mouse anti-GD2 monoclonal antibody to its target.

Results: Post-treatment sera from 7 of 12 dogs developed CAHA levels over pre-treatment that were identified by ELISA as significant increases at Day 30 and/or Day 60. Day 10, Day 30, and Day 60 post-treatment sera from 10 of 12 dogs significantly inhibited the binding of anti-GD2 monoclonal antibody to its target compared to pre-treatment. Significant binding inhibition was also detected in 2 of 12 dogs after local RT but before IT-IC (Day 1). Normal canine sera did not mediate binding inhibition.

Conclusions: This study advances CAHA detection strategies and reports the kinetics of CAHA following IT-IC in dogs with spontaneous melanoma.

Introduction

Companion (pet) dogs with spontaneous tumors provide unique and clinically relevant insights into human tumor biology, therapy, and drug development [1, 2]. Dogs develop spontaneous tumors, similar to humans [3]. This contrasts with many laboratory mouse models where tumors are experimentally induced [4]. Moreover, the molecular and genetic characteristics of many canine cancers resemble those of human cancers [5]. While no model perfectly recapitulates human cancer, the companion dog melanoma patient population holds a distinctive position in oncology research and has received attention from the scientific community as being somewhat parallel to human melanoma patients, particularly for evaluation of immunotherapy studies [6-10]. In that regard, development of antidrug antibodies (ADAs) against immunotherapeutic monoclonal antibodies (mAbs) is well documented in human patients, and the presence of ADAs can impact the safety and efficacy of immunotherapy [11-15]. Moreover, the immune response is highly species-specific and relatively few immunotherapeutic mAbs are caninized, i.e., canine speciated [16]. Therefore, it will be critical to monitor ADAs in the setting of canine immunotherapy, particularly when the immunotherapeutic is a mAb of a species ‘foreign’ to the dog (e.g., a humanized mAb).

The humanized mAb Hu14.18-IL2 and the chimeric ch14.18-IL2, both GD2-targeting mAbs linked to IL2 and known as immunocytokines (IC), have been studied *in vitro* and in preclinical mouse models with GD2-expressing tumors [17-20]. Clinical trials evaluating intravenous (IV) delivery of hu14.18-IL2 IC in patients with melanoma or neuroblastoma have demonstrated immune activation and had manageable safety

87 profiles [21-25]. Although hu14.18-IL2 is a humanized mAb, some patients still
88 developed antibodies to the therapeutic IC [22, 26]. In these patients, antibodies were
89 detected to both the idiotype, i.e., the antigen binding end, and the Fc-IL2 end of the IC
90 [22, 26]. A substantial fraction of patients develop a detectible anti-IC antibody
91 response, and some patients develop a strong anti-IC response and functional, in vivo
92 "neutralization" of detectible IC. Namely, following detection of a strong anti-IC
93 response, blood obtained immediately after an IC infusion does not contain the
94 anticipated level of detectible IC, based on the IC level in the blood obtained from
95 samples collected prior to development of the anti-IC response [22, 26]. A neutralizing
96 anti-human antibody (HAHA) or anti-chimeric antibody (HACA) has been reported for
97 some patients treated with humanized or chimeric hu14.18 mAb [27, 28].

98 The immunogenicity of the humanized hu14.18-IL2 is potentially a greater
99 concern when administering this molecule to a "foreign" species, e.g., to a mouse or
100 dog, as ADAs could interfere with the pharmacokinetics of this therapy, potentially
101 reducing its efficacy [29]. When huKS1/4-IL2, a humanized antibody directed against
102 the human epithelial cell adhesion molecule, was administered intravenously to mice
103 with adenocarcinoma, the mice mounted significant ADAs in the form of mouse anti-
104 human antibodies (MAHAs) resulting in rapid clearance of additional doses of the
105 therapeutic [18]. Delivering hu14.18-IL2 intratumorally in mouse models also induced a
106 MAHA response, similar to what was seen following IV-IC therapy [30]. In addition,
107 ADAs in dogs have been observed in other studies, including one report following
108 subcutaneous administration of a therapeutic IC [31-33]. However, the development of

109 canine anti-human antibodies (CAHAs) following intratumoral immunotherapy with an IC
110 has not been reported.

111 Here we present CAHA assay development and CAHA monitoring of companion
112 dogs with spontaneous melanoma enrolled in a clinical trial of local RT plus intratumoral
113 hu14.18-IL2. An in-house ELISA was developed and used to monitor CAHA against the
114 IgG portion of the IC. Previous studies have demonstrated the ability of ELISA to detect
115 ADAs against antibody-based biopharmaceuticals [26, 34-37]. Our ELISA is
116 customizable, cost-effective, and uses common laboratory reagents and equipment. We
117 also examined if CAHA interferes with the ability of the GD2-binding mAb part of the IC
118 to recognize GD2 in a cell-based flow cytometry assay. Details about safety, clinical
119 activity, and tumor biopsy analyses from this trial, as well as another trial, are separately
120 reported [38, 39].
121

122 Material and Methods

123 Trial eligibility and enrollment

124 Client-owned companion (pet) dogs weighing ≥5 kg with a readily palpable and
125 accessible oral malignant melanoma (histologically confirmed) of at least 2.0 cm
126 (longest diameter) were included in the study. Both treatment naïve dogs and dogs with
127 surgically recurrent tumors were allowed, provided the recurrence met the minimum
128 size criteria. All dogs were required to have a pretreatment constitutional clinical sign
129 status of 0 or 1 (normal or mild lethargy over baseline; diminished activity from pre-
130 disease level but able to function as an acceptable pet) according to VCOG-CTCAE v2

131 criteria at study entry [40]. Dogs determined to have any significant co-morbid illness
132 were excluded.
133

134 Study design

135 Client-owned companion dogs with locally advanced or metastatic melanoma
136 were randomized to receive either a single 8 Gy fraction (Arm A) or three 8 Gy fractions
137 delivered over 1 week (Arm B) to the primary site and regional lymph nodes (when
138 clinically involved) with the single or last fraction 5 days prior to IT-IC at 12 mg/m^2 on 3
139 consecutive days. Prior to treatment, a baseline physical examination with tumor
140 measurements was performed, blood was collected for clinical assessments, and blood
141 was collected for banking of serum, plasma, and peripheral blood mononuclear cells
142 (PBMC) for subsequent *in vitro* analysis. External beam radiation therapy (RT) was
143 delivered by image-guided intensity modulated radiation using helical tomotherapy
144 (TomoTherapy HiArt Treatment System, Accuray Inc., Sunnyvale, CA, USA). The
145 hu14.18-IL2 was provided as lyophilized vials (4 mg/vial; each ml prior to lyophilization
146 contained 4 mg/ml hu14.18-IL2, 2% sucrose, 80mM L-arginine, 10mM citric acid, 0.2%
147 polysorbate 20, pH 5.5) and was reconstituted with either 0.5 ml or 0.25 ml 0.9% (w/v)
148 NaCl for injection at a concentration of either 8 mg/ml or 16 mg/ml. The total volume
149 was administered using multiple needle re-directions into the target lesion within and
150 surrounding the lesion. Injections were performed on 3 consecutive days. PBMC were
151 obtained at pre-treatment and various times post-treatment. The treatment schema and
152 blood collection times are shown in Fig 1.
153

154 **Fig 1. Treatment Schema.** All dogs receive radiation therapy (RT) to the local site
155 either in 1x 8 Gy (Arm A) or 3x 8 Gy fractions over 1 week (Arm B). RT was delivered on
156 Day -4 (Arm A) or on Days -8, -6 -4 (Arm B). Intratumoral (IT) injection of IC is
157 administered (IT-IC) on three consecutive days starting five days after completion of RT.
158 All days were allowed ± 1-2 days leeway for flexible scheduling around holidays, subject
159 vacations, and clinic scheduling.
160

161 ## IACUC approvals

162 The authors confirm that the appropriate ethical review committee approval has
163 been received. All procedures and treatments performed on client-owned companion
164 dogs were approved by the Institutional Animal Care and Use Committees of the
165 University of Wisconsin-Madison School of Veterinary Medicine (Approval V006037)
166 and by the Animal Care Committee at the William S. Middleton Memorial Veterans
167 Hospital. Written informed consent was obtained from all companion dog caregivers
168 prior to entry into this trial. Protocol treatments were administered at the University of
169 Wisconsin Veterinary Care (UWVC) hospital.
170

171 ## Canine Anti-Human ELISA

172 A standard protocol was adapted to develop an ELISA to detect canine
173 antibodies against human IgG [41]. Nunc MaxiSorp™ Flat-Bottom 96-well plates
174 (Thermo Scientific Inc., USA) were coated with ChromPure Human IgG (Jackson
175 ImmunoResearch Laboratories, Inc., USA) [10μg/mL, 50μL/well in ELISA Coating Buffer
176 (Bio-Rad Laboratories, Inc., USA)], which served as the “capture” agent, and incubated

177 overnight at 4°C. The coating solution was removed, and the wells washed three times
178 (3x) with distilled water (DI). The plate was blocked with Neptune™ Block
179 (ImmunoChemistry Technologies, USA) (200µL/well) for 1 hour at 25°C followed by
180 washing as above. Canine serum was diluted 1:20 in PBS and added to wells in
181 quadruplicate at 50µL/well and incubated for 1 hour at 25°C. A murine mAb against
182 human IgG (ab436, Abcam, USA) was used as a positive control, as we are not aware
183 of any commercially available canine anti-human IgG to serve as a positive control. The
184 mAb was diluted 1:1,000 in PBS and added to wells in quadruplicate at 50µL/well and
185 incubated for 1 hour at 25°C. PBS was added to wells as a negative control. Wells were
186 washed as above. Rabbit anti-mouse IgG (H+L) antibody, affinity purified against human
187 serum proteins conjugated to horseradish peroxidase (HRP) (# 315-035-045, Jackson
188 ImmunoResearch Laboratories Inc., USA) was the secondary (i.e.: "detection") antibody,
189 was diluted 1:40,000 in PBS, added to wells at 75µL/well, and incubated for 30 minutes
190 (min.) at 25°C. Wells were washed as above. The plate was developed with1-Step™
191 Ultra TMB-ELISA solution (Thermo Scientific Inc., USA) (75µL/well) and incubated for
192 15 min. at 25°C. The reaction was stopped by addition of TMB stop solution (Sera Care,
193 USA) (75µL/well), and the absorbance at 450nm read on a SpectraMax M3 Micro-Plate
194 reader.
195

196 ## Cell culture

197 The GD2+ M21 human melanoma cell line was cultured in RPMI-1640
198 supplemented with 10% fetal bovine serum (GeminiBio, BenchMark™), 25 mM HEPES,
199 2 mM L-glutamine, 1 mM sodium pyruvate, and 1X non-essential amino acids

200 (Mediatech). M21 was obtained as a gift from Dr. Ralph Reisfeld (Scripps Research
201 Institute, La Jolla, CA, USA).
202

203 Detection of GD2 binding inhibition by CAHA using flow
204 cytometry

205 Mouse anti-GD2 mAb 14G2a-PE (BioLegend, #357303) (100 μl) was added to
206 2.5 μl canine sera from this study (Baseline, Day 1, Day 10, Day 30, Day 60) or to
207 serum from healthy dogs (2.5 μl or 20 μl) (Antibodies Inc, #54-490-0005) and adjusted
208 to a total volume of 120 μl using 1% FBS/PBS flow cytometry wash buffer (WB). A
209 sample without canine sera was used as a staining control. The light-protected mixture
210 was incubated for 30 min. at 4°C. The serum-14G2a mixture was added to GD2+ M21
211 cells aliquoted to flow cytometry tubes and incubated for 30 min.at 4°C, followed by 2x
212 washes with WB. Cells were fixed with Cytofix Fixation Buffer (BD, #554655) for 15 min.
213 at 25°C, washed 1x with WB, resuspended in WB, and held at 4°C until analysis. Data
214 were acquired on a BD LSR Fortessa, single cells were gated, and the Median
215 Fluorescence Intensity (MFI) was determined with FlowJo™ Software (BD Life
216 Sciences). Binding inhibition was calculated as follows where X equals Day 1, Day 10,
217 Day 30, or Day 60:

218 $$\%\ \text{Binding Inhibition} = 100 \times \frac{\text{Baseline MFI} - \text{Day X MFI}}{\text{Baseline MFI}}$$

219

220 Statistical Analysis and Considerations

221 Animal specific kinetic levels of CAHA following IT-IC were summarized in terms of
222 means and standard errors. Profile plots were generated to examine changes over time.
223 Changes from baseline to Day 10, 30, and 60 were evaluated using a generalized linear
224 model. Model assumptions were validated by examining residual and normal
225 probabilities plots. Dunnett's test was used to control the type I error (<0.05) when
226 conducting multiple comparisons for changes from baseline to Day 10, 30, and 60. All
227 reported P values are two-sided and P<0.05 was used to define statistical significance.
228 Statistical analyses were conducted using SAS software (SAS Institute, Cary NC),
229 version 9.4. Plots were generated using R software version 4.2.1 with graphical
230 packages [42-44].
231

232 Results

233 Companion dog characteristics

234 Twelve dogs met eligibility criteria for the trial and were enrolled and randomized into
235 one of the two treatment groups from May 2020 to December 2021 [38]. Companion
236 dog breed, tumor characteristics, and randomization results are summarized in Table 1.
237 All 12 dogs completed the treatment phase of the protocol, and none experienced
238 significant or unexpected adverse events [38].
239

Table 1. Characteristics and status of dogs receiving 12 mg/m^2 IC and randomized to RT Arm A or RT Arm B

Patient ID	Breed	Sex	Age (yr)	Wt (kg)	Tumor Site & Stage at Diagnosis	RT Arm[a]	Sera assayed from all timepoints?

ITIC-04	Labrador Retriever	SF	10	38.9	Left Maxilla/Pulmonary nodule (T2N0M1)	A	Yes
ITIC-05	Burnese Mountain	NM	7	43.4	Right hindlimb subcutaneous (T2N2M0)	B	Yes
ITIC-06	Min. Poodle mix	NM	10	6.6	Right Mandible (T2N1M0)	A	No[b]
ITIC-07	Aust. Cattle mix	NM	13	31.2	Left Maxilla (T2N0M0)	B	Yes
ITIC-08	Beagle mix	NM	11	15.8	Soft palate (T2N1M0)	B	Yes
ITIC-09	Great Dane	SF	10	51.7	Left Maxilla (T2N1M1)	A	Yes
ITIC-10	German Shepherd	NM	9	26.3	Right Maxilla (T2N0M0)	A	Yes
ITIC-11	Mix Breed	NM	11	26.5	Right Mandible (T2N0M1)	B	Yes
ITIC-12	Pom mix	SF	11	9.0	Left Maxilla (T3N1M0)	A	No[b]
ITIC-13	Mix Breed	NM	10	7.0	Cutaneous (TxN1M1)	A	Yes
ITIC-14	Collie mix	SF	11	25.0	Left Maxilla (T2N1M0)	B	Yes
ITIC-15	Mix Breed	NM	9	36.1	Lingual (T2N0M0)	B	Yes

IC, immunocytokine; RT, radiation therapy; SF, spayed female; NM, neutered male
[a]Arm A, a single 8 Gy fraction to the primary tumor followed 5 days later with hu14.18-IL2 IC (12 mg/m^2 for 3 consecutive days); Arm B, three 8 Gy fractions delivered on a Monday, Wednesday and Friday schedule followed 5 days later with hu14.18-IL2 IC (12 mg/m^2 for 3 consecutive days).
[b]Serum not available from Day 60.

Detection of CAHAs by ELISA

We developed an in-house sandwich ELISA to detect antibodies in canine sera specific to human IgG — the antibody portion of hu14.18 is humanized IgG. For this assay to work, a secondary antibody specific for, or cross-reactive to, canine

245 immunoglobulin is required. Additionally, to avoid the need for multiple secondary
246 reagents, reactivity to mouse immunoglobulin, the species the positive control is raised
247 in, was preferred. We first tested our potential secondary reagents by optimizing their
248 ability to generate a strong signal when detecting mouse anti-human IgG mAb as the
249 positive control (in place of the canine serum), as the mouse anti-human IgG was
250 serving as the positive control reagent, namely the analyte. Our initial “checkerboard”
251 trials tested various concentrations of human IgG coating antigen, mouse anti-human
252 IgG mAb as the analyte, and rabbit anti-dog HRP secondary antibody. As expected, the
253 measured absorbance was dependent on the concentration of the rabbit anti-dog HRP
254 secondary, i.e., absorbance decreased as concentration of the secondary decreased. In
255 contrast, the absorbance was not dependent on the concentration of either the coating
256 human IgG or the mouse anti-human IgG mAb (data not shown). To address these
257 issues, we first troubleshot reagents and/or steps, e.g., testing different blocking buffers,
258 including 5% normal rabbit sera, as well as non-mammalian protein buffers, increasing
259 the blocking time, and testing different wash buffers. These changes did not resolve the
260 high background issue, which was also observed in negative control wells, i.e., in wells
261 incubated with PBS instead of the mouse anti-human IgG mAb.

262 These data suggested that the rabbit anti-dog HRP secondary may be binding to
263 the human IgG coating on the plate. Immunoglobulins from different species share
264 similar protein structures [41]. Therefore, antibodies against one species are likely to
265 cross-react with a number of other species — a property which, as discussed below,
266 was leveraged to optimize the assay. We adsorbed the rabbit anti-dog secondary
267 antibody with excess human IgG; however, recognition of human IgG by this adsorbed

268 reagent was only slightly minimized (data not shown). We are not aware of a
269 commercially available anti-dog secondary antibody adsorbed to human serum proteins.
270 Using the cross-reactivity of different species' immunoglobulins, we next tested a
271 commercially available rabbit anti-mouse IgG secondary antibody adsorbed to ensure
272 minimal cross-reactivity with human serum proteins. The human adsorbed rabbit anti-
273 mouse IgG did not bind to plate-bound human IgG while the cross-reactivity to the
274 positive control mouse IgG was maintained. This one reagent then permitted the use of
275 a single secondary antibody to effectively detect both CAHA and mouse-anti-human
276 antibody (MAHA).

277 Post-treatment sera from seven of twelve dogs tested positive for anti-human IgG
278 antibodies determined via our in-house CAHA ELISA (Fig 2). Pre-treatment sera was
279 used as baseline and as an internal control for each dog's post-treatment samples. Two
280 of six and five of six dogs in Arm A and Arm B, respectively, demonstrated significant
281 increases in anti-human IgG compared to the pre-treatment absorbance (Fig 2). The
282 post-treatment anti-human IgG was significantly increased compared to pre-treatment
283 anti-human IgG at Day 30 for five dogs and at Day 60 for five dogs. For Arm A, both
284 samples reaching significance were from Day 30 (K906 and K909). The sera from
285 K909 no longer had a significant increase in CAHA at Day 60 and no sera was available
286 for Day 60 CAHA analysis from K906. For Arm B, anti-human IgG antibody levels in
287 three dogs were elevated similarly at Day 30 and Day 60 (K905, K911, K915), one dog
288 had an elevated level at Day 30 that declined by Day 60 (K914), and one had an
289 elevated level that was only detected at Day 60 (K908). No dogs had detectable anti-
290 human IgG antibodies following RT but before IT-IC (Day 1) or at Day 10 post-

291 treatment. There were no substantial differences in anti-human IgG levels between
292 negative control wells with PBS only and pre-treatment samples for the 12 dogs
293 enrolled in this study.
294
295 **Fig 2. CAHA is induced in some dogs receiving IT-IC injections.** Mean CAHA levels,
296 measured as O.D. values by ELISA, from sera assayed in quadruplicate collected at
297 Baseline (before radiation), Day 1 (after radiation, but prior to IT-IC), and Days 10, 30
298 and 60 (after IT-IC) with standard deviation error bars are shown. Day 60 timepoint was
299 not available for two dogs, K906 and K912, in Arm A. Increases in absorbance from
300 Baseline to Day 1, Day 10, Day 30, or Day 60 for each dog were analyzed and
301 significance indicated as * $p < 0.05$; ** $p < 0.01$; *** $p < 0.001$.
302

303 Sera from dogs treated with hu14.18-IL2 inhibit in vitro
304 binding to GD2

305 We modified a flow cytometry assay to determine the potential for CAHA in
306 canine sera to inhibit the binding of IC to GD2 on cells [30]. In this assay, sera are first
307 incubated with 14G2a-PE, a mouse mAb that recognizes GD2 at a dilution of ~1:48.
308 The mixture is subsequently added to GD2+ M21 cells, and the level of PE fluorescence
309 is determined. 14G2a is an IgG2a-class switch variant of the mouse IgG3 mAb clone
310 14.18, and thus has the same idiotype as that of the humanized immunocytokine
311 hu14.18-IL2 [45]. Consequently, some of the CAHA in dog sera that recognizes 14G2a
312 may in effect recognize the idiotype shared by 14G2a and hu14.18-IL2, while some of
313 the CAHA might also recognize other regions of the IC. Thus, in this assay, the PE

314 fluorescence of the 14G2a-PE mAb bound to the M21 cells will be decreased if any of
315 the CAHA sin sera from treated subjects recognize the idiotype of 14G2a and effectively
316 block its binding to GD2 on the M21 cells. In contrast, substantial PE fluorescence will
317 be detected if the serum antibodies do not block the binding of 14G2a to GD2.

318 In preliminary experiments, we assayed healthy canine sera for components in
319 dog serum that might interfere with the flow cytometry assay. Serum is a complex
320 biologic that contains carbohydrates, proteins, and lipids that can interfere with the
321 ability of antibodies to bind their targets. Healthy serum was spiked into PBS and
322 incubated with the 14G2a anti-GD2 mAb before adding the mixture to M21 cells, as
323 described above. Compared to M21 stained in the absence of healthy sera, the addition
324 of sera substantially inhibited 14G2a binding to GD2 in a concentration dependent
325 manner. Substantial inhibition (~50.2%) was observed at 1:6 ratio of normal sera to PBS
326 whereas at a 1:48 ratio inhibition was largely undetected (> 0.1%) (S1 Fig). As the
327 observed interference of healthy control serum on 14.G2a-PE binding to M21 was
328 ameliorated at the 1:48 ratio, we used this same ratio to test sera from the clinical trial.
329 We included heathy donor sera diluted 1:6 and 1:48 with PBS as positive and negative,
330 respectively, controls in each assay. Each dog's pre-treatment sample was used as its
331 baseline.

332 Varying levels of binding inhibition were observed in 10 of 12 dogs (all but K913
333 and K914) when canine sera were mixed with 14G2a mAb before the mixture was used
334 to stain M21 cells (Table 2, Fig 3, and S2 Fig for select data). The binding was
335 significantly inhibited at Days 10, 30 and 60 compared to pre-treatment in all 10 of these
336 same dogs (save for subjects K906 and K912, that did not have day 60 serum sample

collected). GD2 binding was also significantly inhibited by Day 1 sera from 2 of these same 10 dogs, one dog in each Arm, (K910 and K915), but for these 2 dogs, the calculated binding inhibition on Day 1 was not as high as at any of the other days tested for those same 2 dogs. In the remaining 10 dogs, that did not have significant binding inhibition on Day 1, the binding of 14G2a to GD2 was increased at Day 1 for 8 of them (all but K905 and K908), i.e., the % inhibition calculated using the formula in the methods section was negative, corresponding to a slight increase in binding at Day 1 compared to the pre-treatment serum. However, the increase in binding seen on Day 1 (i.e., the negative binding inhibition value) was significant in only one of these eight dogs (K909) (median -8.7%, range -0.3 to -21.2%) (Fig 3 and Table 2). These relatively small positive or negative binding inhibition values detected on Day 1 (prior to any IT-IC treatment, but after RT), which are significant only for 3 dogs (two positive and one negative), were not anticipated and are discussed below; for all 3 of these dogs, all 3 subsequent time points for each dog show higher and statistically significant binding inhibition. In contrast to the 10 dogs that did show significant binding inhibition, sera from the other 2 dogs (K913 and K914), did not inhibit GD2 binding at any timepoint (Fig 3 and Table 2). Select flow cytometry data are shown in S2 Fig.

Table 2. Binding Inhibition (%) of anti-GD2 mAb to GD2 target in the presence of canine serum

Patient ID	RT Arm	Day 1	Day 10	Day 30	Day 60
ITIC-04	A	-7.6	88.3	98.2	57.2
ITIC-05	B	-1.5	92.8	96.6	98.8
ITIC-06	A	-3.5	74.2	97.3	n/a
ITIC-07	B	-5.6	12.5	91.3	40.6
ITIC-08	B	-0.3	26.4	96.4	89.9

ITIC-09	A	-21.2	93.3	96.1	97.0
ITIC-10	A	17.3	36.1	91.4	53.2
ITIC-11	B	-9.7	23.1	47.1	34.0
ITIC-12	A	-10.4	37.0	91.0	n/a
ITIC-13	A	-11.0	-23.2	-0.6	-6.9
ITIC-14	B	-10.7	13.1	10.2	14.6
ITIC-15	B	12.5	20.9	85.9	75.8

mAb, monoclonal antibody; RT, radiation therapy
Fluorescently labelled anti-GD2 antibody was incubated with canine serum and then used to stain GD2+ M21 tumor cells. % Binding Inhibition of post-treatment samples compared to baseline samples was determined by flow cytometry as described in Materials and Methods.

355

356 **Fig 3. In vitro inhibition of binding of anti-GD2 antibody to GD2 target.** The %
357 binding inhibition at various timepoints compared to Baseline. Data shown are
358 calculated from the mean of triplicates as described in Materials and Methods. Sera was
359 collected at Baseline (before radiation), Day 1 (after radiation, but just prior to IT-IC),
360 and Days 10, 30 and 60 (after IT-IC). Timepoints for each dog are presented and
361 connected by a line. Day 60 timepoint was not available for two dogs, K906 and K912,
362 in Arm A. Significance indicated is based on mean of triplicates at Baseline compared to
363 post-treatment timepoints, * $p < 0.05$; ** $p < 0.01$; *** $p < 0.001$.

364

365 Comparison of CAHA Detection by ELISA and binding 366 inhibition by *in vitro* flow cytometry assay

367 Significant CAHA at various timepoints was detected by ELISA in 7 of 12 dogs: i)
368 K906 and K909 from Arm A at Day 30; ii) K908 from Arm B at Day 60; iii) K914 from Arm
369 B at Day 30; and iv) K905, K911, and K9 15 from Arm B at Day 30 and Day 60 (Fig 2).

370 Except for the Day 30 sera from K914, the above sera also significantly inhibited 14G2a
371 from binding to GD2 in the flow cytometry assay (Fig 3). To evaluate the relationship
372 between the ELISA and binding inhibition, the values for each serum sample for each
373 subject are plotted in Fig 4, with the ELISA O.D. value plotted on the Y axis, and the %
374 binding inhibition value plotted on the X-axis. There were no significant correlations
375 between the two assays within or for both arms combined detected. Significant binding
376 inhibition was detected earlier than significant CAHA: i) at Day 1 in 2 dogs; and ii) at
377 Day 10 in 10 dogs. Overall, inhibition was detected in 10 of 12 dogs: i) 5 of 6 Arm A
378 dogs and 5 of 6 Arm B dogs at Day 10; ii) 5 of 6 Arm A dogs and 5 of 6 Arm B dogs at
379 Day 30; iii) 3 of 4 Arm A dogs and 5 of 6 Arm B dogs at Day 60. Sera from the two dogs
380 that did not inhibit binding in the flow cytometry assay (K913 and K914) were also
381 CAHA negative by ELISA except for the Day 30 sera from K914 (Figs 2 and 3). Healthy
382 canine sera at the same dilution as sera from the clinical trial dogs were negative for
383 CAHA and did not inhibit the binding of 14G2a to M21 (Fig B in S1 Fig).
384
385 **Fig 4. The relationship of CAHA and binding inhibition by *in vitro* flow cytometry**
386 **assay.** The % binding inhibition related to CAHA at various timepoints is shown.
387 Timepoints for each dog are presented. Timepoints with significant CAHA responses are
388 shown with significance indicated, these timepoints also had significant binding
389 inhibition except for K914 Day 30. Sera from 10 of 12 dogs significantly inhibited binding
390 of anti-GD2 antibody to GD2 target at Day 10, 30 and 60 with the exceptions of K913
391 (shown as open symbols) and K914 (shown as black symbols). Day 1 sera from two

392 dogs (K910 and K915) inhibited binding. A single serum sample, K914 Day 30, showed
393 a significant CAHA response but did not inhibit binding (shown as the black circle).
394

395 # Discussion

396 We developed two distinct assays to monitor and assess the CAHA response in
397 dogs receiving treatment of a readily palpable oral malignant melanoma with local RT
398 plus IT injection of a humanized IC. An ELISA was designed to detect CAHAs
399 specifically targeting human IgG – which is analogous to the Fc portion of hu14.18-IL2
400 [45]. We also utilized a flow cytometry assay to investigate the inhibition of anti-GD2
401 mAb binding to GD2 by sera from dogs receiving RT and IT-IC. This approach
402 employed ELISA as a tool to identify the presence of ADA in serum, followed by a
403 subsequent flow cytometry analysis to provide additional characterization of the ADA
404 response.

405 Although there are commercially available assays to detect various anti-species
406 antibodies, e.g., mouse anti-human (MAHA) and human anti-mouse (HAMA), an off-the-
407 shelf assay is not available to detect CAHA. The absence of a commercially available
408 ELISA specifically designed to detect CAHAs is an unmet need within the comparative
409 immuno-oncology field. This gap becomes increasingly relevant as the canine model
410 gains recognition for its value in studying human disease. The primary objective of
411 developing our in-house CAHA ELISA was to create a monitoring tool that would be
412 easy to use in veterinary and translational research laboratories. Additionally, we sought
413 to develop a cost-effective and flexible assay. The binding specificity of the CAHA could

414 also be explored in more depth by modifying the whole human IgG coating reagent that
415 was used in this report (e.g., whole IgG, Fc fragment, Fab or $F(ab')_2$).

416 A challenge in developing an ELISA to detect canine antibody that binds human
417 IgG was the lack of commercially available anti-canine IgG HRP conjugates that were
418 cross absorbed against human IgG. This cross-absorption step is crucial for reducing
419 the assay background and ensuring specificity. To address this limitation, we used a
420 rabbit anti-mouse IgG HRP conjugate that had been cross absorbed against human
421 IgG. Our testing during assay optimization demonstrated sufficient cross-reactivity
422 between mouse and canine-derived IgG, enabling us to detect CAHA to human IgG
423 (data not shown). In addition, we included a commercially available mouse IgG specific
424 for human IgG as a control analyte sample for detection by the rabbit anti-mouse HRP
425 in each assay. The selection of antibodies and the incorporation of cross-absorption
426 steps contributed to the assay's specificity and adaptability for potential use in both
427 veterinary and translational research lab settings.

428 Our CAHA ELISA is primarily designed to detect free ADAs in serum, by
429 detecting their binding to plate-bound human IgG. In contrast, the in vitro binding
430 inhibition flow cytometry assay allows the ADAs to interact with the soluble mouse
431 14.G2a mAb (which shares the idiotype of the hu14.18-IL2 IC) in solution, and
432 evaluates detection of GD2 binding in a cellular context, enabling the detection of ADAs
433 that inhibit or interfere with the binding of a therapeutic drug to its specific target in its
434 natural form on the cell surface, e.g., GD2 on tumor cells. This distinction is critical
435 because antigens immobilized to plastic, as in an ELISA, may not accurately mimic the

436 natural conformations of antigens on cell surfaces [46], potentially leading to an
437 underestimation of certain ADAs by this ELISA that flow cytometry can detect.

438 It is of interest that two dogs (K910 and K915) inhibited the binding of the anti-
439 GD2 mAb to GD2 on target cells at Day 1. The Day 1 sample was collected the day of,
440 but prior to, the first injection of hu14.18-IL2. Therefore, these responses following RT
441 may reflect pre-existing canine anti-human or anti-mouse antibodies, cross species-
442 reactive antibodies, or assay interference [47-49]. The first step in the flow cytometry
443 binding inhibition assay is the incubation of canine sera with the mouse anti-GD2 mAb
444 14G2a prior to incubating the mixture with the GD2+ M21 cells. Therefore, a possible
445 explanation for the Day 1 binding inhibition is pre-existing canine anti-mouse antibodies
446 as previously reported [48], but these would have needed to appear, or be boosted,
447 following baseline, as the positive binding inhibition is detected in comparison to the
448 baseline value for that same dog. We did not prospectively survey clients regarding their
449 pet's known allergies or exposures to other mammalian species, e.g., mouse or rabbit,
450 which could potentially induce a humoral response. mAbs of both mouse and rabbit
451 origin are used in our in-house assays and could result in assay background or
452 interference. However, neither of these two dogs were CAHA+ by ELISA at Day 1. Anti-
453 human IgG was not detected by ELISA until Day 30 in any dog, nor from healthy canine
454 sera, suggesting exposure to hu14.18-IL2 as the origin of the antibodies. However, we
455 have not formally tested for pre-existing anti-mouse or anti-rabbit antibodies in these
456 dogs. These seemingly discordant data could reflect the different assay sensitivities and
457 different assay modalities. Moreover, serum from healthy humans and healthy dogs can

458 both contain detectable levels of autoantibodies including rheumatoid factors and anti-
459 idiotypic antibodies which may cause assay interference [47, 49, 50].

460 Additionally, activation of B cells, generation of anti-tumor antibodies and
461 establishment of B cell memory following a treatment regimen similar to that used in this
462 trial have been reported in a mouse melanoma model [51]. As IgM typically arises early
463 in an immune response, the CAHA response detected at early timepoints (e.g., Day 1,
464 Day 10) in this study may be of IgM isotype which our CAHA ELISA may also detect. in
465 contrast, the flow cytometry assay does not detect a particular antibody isotype and
466 thus may detect ADA despite lack of CAHA detected by ELISA in the same serum. The
467 detection of binding inhibition at early time points may also result from the isotype
468 agnostic nature of the flow cytometry assay. The increase in binding inhibition observed
469 in two dogs (K910 and K915) from baseline to Day 1 was unexpected as the dogs had
470 not been exposed to hu14.18-IL2 at the time of serum collection on either day.
471 Moreover, the timeframe from baseline to Day 1 in this study was between 5-9 days,
472 representing rapid kinetics for a *de novo* humoral response. However, we have not
473 determined the fine specificity of the antibody responses in this study. All dogs treated
474 in this study received radiation, thus there is potential for radiation-induced antigen
475 shedding by tumor to trigger a humoral response [52]. Tumor-specific and self-specific
476 antibodies have been found in sera of cancer patients in several studies [53, 54]. Thus,
477 the binding inhibition at Day 1 in these two dogs could be due to endogenous cross-
478 reactive antibodies or those recognizing cryptic epitopes or neoantigens [55].

479 The IC has humanized IL2 linked to the mAb Fc region, thus the IL2 and/or the
480 linker between the Fc and the IL2 may be recognized as foreign in the dog triggering an
481 immune response. None of the dogs in this study experienced significant or unexpected
482 adverse events [38]. However, as dogs received only a single 3-day course of IT-IC, we
483 could not evaluate the impact of induced ADAs on subsequent pharmacokinetics of
484 hu14.18-IL2 or on the potential toxicity during subsequent courses. It will be important to
485 evaluate peak serum levels of hu14.18-IL2 as well as monitor anti-IL2 and anti-linker
486 responses to determine if CAHA+ sera affect antibody-mediated cellular cytotoxicity, as
487 seen in some humans receiving IC treatment [26].

488 Additional studies could further characterize the binding specificity in terms of
489 distinct IgG regions, e.g., Fc receptor, Fab hinge region [48]. Further, as in humans, IgG
490 is the most prevalent Ig in canine sera, however IgM and IgA are present at lower
491 concentrations [56]. The rabbit anti-mouse IgG HRP secondary reagent used in the
492 ELISA is reactive to both the heavy and light chain of mouse IgG. As such, this reagent
493 may also react with other immunoglobulin classes, e.g., IgM, IgA, since these all share
494 the same light chain. Therefore, subsequent testing could determine the isotype of the
495 CAHA responses, as well as species cross-reactivity – in particular to mouse or rabbit
496 IgG.

497 The timeline of the anti-human IgG CAHA ELISA response observed in our study
498 (7 of 12 dogs at Day 30) is similar to that observed in a previous study of dogs treated
499 with NHS-IL12, a humanized antibody against necrotic tumor regions linked to
500 humanized IL12. Dogs treated with NHS-IL12 developed ADA against both human IgG

501 (8 of 12 dogs) and against human IL12 (5 of 14 dogs) between 15 to 29 days after
502 treatment [31]. Factors that may explain differences in the ADA timeline between our
503 study and that of Paoloni et al., include the composition and target of the IC, IC dose
504 level, administration route, as well as the assays used to monitor the development of
505 ADA.

506 Conclusion

507 The CAHA detection assays in this report provide tools to monitor parallel canine
508 patient populations receiving treatment with human biopharmaceuticals. These assays
509 should be translatable to other treatment regimens delivering “foreign” protein
510 molecules *in vivo*, as well as to species other than the dog, provided appropriate
511 controls are available. The recent availability of immune checkpoint blockade in the form
512 of a caninized anti-PD1 therapeutic mAb (Gilvetmab, Merck) expands the treatment
513 options for dogs with melanoma. To this end, we are evaluating the addition of immune
514 checkpoint blockade, i.e., anti-PD1, to our novel treatment regimen of RT and IT-IC with
515 hu14.18-IL2 in dogs with melanoma. Local anti-tumor responses as well as systemic
516 immune responses, including the development of CAHA using the assays described
517 herein, will be investigated.

518 Acknowledgements

519 We are grateful for the dogs with melanoma, their caregivers, and referring
520 veterinarians who participated in the clinical trial. We are also thankful for the healthy
521 dogs and their caregivers for donating peripheral blood samples. We thank Rubi Hayim,

522 Emily M. Tomesek, and the UW Veterinary Care Oncology team for caring for the dogs
523 in this study.

524 # References

525 1. Gardner HL, Fenger JM, London CA. Dogs as a Model for Cancer. Annu Rev
526 Anim Biosci. 2016;4:199-222. Epub 20151109. doi: 10.1146/annurev-animal-022114-
527 110911. PubMed PMID: 26566160; PubMed Central PMCID: PMCPMC6314649.
528 2. Paoloni M, Khanna C. Translation of new cancer treatments from pet dogs to
529 humans. Nat Rev Cancer. 2008;8(2):147-56. doi: 10.1038/nrc2273. PubMed PMID:
530 18202698.
531 3. Vail DM, MacEwen EG. Spontaneously occurring tumors of companion animals
532 as models for human cancer. Cancer Invest. 2000;18(8):781-92. doi:
533 10.3109/07357900009012210. PubMed PMID: 11107448.
534 4. Onaciu A, Munteanu R, Munteanu VC, Gulei D, Raduly L, Feder RI, et al.
535 Spontaneous and Induced Animal Models for Cancer Research. Diagnostics (Basel).
536 2020;10(9). Epub 20200831. doi: 10.3390/diagnostics10090660. PubMed PMID:
537 32878340; PubMed Central PMCID: PMCPMC7555044.
538 5. Oh JH, Cho JY. Comparative oncology: overcoming human cancer through
539 companion animal studies. Exp Mol Med. 2023;55(4):725-34. Epub 20230403. doi:
540 10.1038/s12276-023-00977-3. PubMed PMID: 37009802; PubMed Central PMCID:
541 PMCPMC10167357.
542 6. Crossley RA, Matz A, Dew T, Kalinauskas A, Faucette N, Poff B, et al. Safety
543 Evaluation of Autologous Tissue Vaccine Cancer Immunotherapy in a Canine Model.
544 Anticancer Res. 2019;39(4):1699-703. doi: 10.21873/anticanres.13275. PubMed PMID:
545 30952708.

546 7. Dow S. A Role for Dogs in Advancing Cancer Immunotherapy Research. Front
547 Immunol. 2019;10:2935. Epub 20200117. doi: 10.3389/fimmu.2019.02935. PubMed
548 PMID: 32010120; PubMed Central PMCID: PMCPMC6979257.
549 8. Maekawa N, Konnai S, Nishimura M, Kagawa Y, Takagi S, Hosoya K, et al. PD-
550 L1 immunohistochemistry for canine cancers and clinical benefit of anti-PD-L1 antibody
551 in dogs with pulmonary metastatic oral malignant melanoma. NPJ Precis Oncol.
552 2021;5(1):10. Epub 20210212. doi: 10.1038/s41698-021-00147-6. PubMed PMID:
553 33580183; PubMed Central PMCID: PMCPMC7881100.
554 9. Park JS, Withers SS, Modiano JF, Kent MS, Chen M, Luna JI, et al. Canine
555 cancer immunotherapy studies: linking mouse and human. J Immunother Cancer.
556 2016;4:97. Epub 20161220. doi: 10.1186/s40425-016-0200-7. PubMed PMID:
557 28031824; PubMed Central PMCID: PMCPMC5171656.
558 10. Zuleger CL, Kang C, Ranheim EA, Kurzman ID, Macklin MD, Newton MA, et al.
559 Pilot study of safety and feasibility of DNA microseeding for treatment of spontaneous
560 canine melanoma. Vet Med Sci. 2017;3(3):134-45. Epub 2017/10/27. doi:
561 10.1002/vms3.65. PubMed PMID: 29067210; PubMed Central PMCID:
562 PMCPMC5645840.
563 11. Davda J, Declerck P, Hu-Lieskovan S, Hickling TP, Jacobs IA, Chou J, et al.
564 Immunogenicity of immunomodulatory, antibody-based, oncology therapeutics. J
565 Immunother Cancer. 2019;7(1):105. Epub 20190415. doi: 10.1186/s40425-019-0586-0.
566 PubMed PMID: 30992085; PubMed Central PMCID: PMCPMC6466770.
567 12. Kim C, Yang H, Kim I, Kang B, Kim H, Kim H, et al. Association of High Levels of
568 Antidrug Antibodies Against Atezolizumab With Clinical Outcomes and T-Cell

569 Responses in Patients With Hepatocellular Carcinoma. JAMA Oncol. 2022;8(12):1825-
570 9. doi: 10.1001/jamaoncol.2022.4733. PubMed PMID: 36264560; PubMed Central
571 PMCID: PMCPMC9585463.
572 13. Sasson SC, Wilkins LE, Watson RA, Jolly C, Brain O, Klenerman P, et al.
573 Identification of neutralising pembrolizumab anti-drug antibodies in patients with
574 melanoma. Sci Rep. 2021;11(1):19253. Epub 20210928. doi: 10.1038/s41598-021-
575 98700-7. PubMed PMID: 34584157; PubMed Central PMCID: PMCPMC8478874.
576 14. Vaisman-Mentesh A, Gutierrez-Gonzalez M, DeKosky BJ, Wine Y. The Molecular
577 Mechanisms That Underlie the Immune Biology of Anti-drug Antibody Formation
578 Following Treatment With Monoclonal Antibodies. Front Immunol. 2020;11:1951. Epub
579 20200818. doi: 10.3389/fimmu.2020.01951. PubMed PMID: 33013848; PubMed Central
580 PMCID: PMCPMC7461797.
581 15. van Brummelen EM, Ros W, Wolbink G, Beijnen JH, Schellens JH. Antidrug
582 Antibody Formation in Oncology: Clinical Relevance and Challenges. Oncologist.
583 2016;21(10):1260-8. Epub 20160720. doi: 10.1634/theoncologist.2016-0061. PubMed
584 PMID: 27440064; PubMed Central PMCID: PMCPMC5061540.
585 16. Klingemann H. Immunotherapy for Dogs: Still Running Behind Humans. Front
586 Immunol. 2021;12:665784. Epub 20210805. doi: 10.3389/fimmu.2021.665784. PubMed
587 PMID: 34421888; PubMed Central PMCID: PMCPMC8374065.
588 17. Hank JA, Surfus JE, Gan J, Jaeger P, Gillies SD, Reisfeld RA, Sondel PM.
589 Activation of human effector cells by a tumor reactive recombinant anti-ganglioside GD2
590 interleukin-2 fusion protein (ch14.18-IL2). Clin Cancer Res. 1996;2(12):1951-9. Epub
591 1996/12/01. PubMed PMID: 9816154.

592 18. Imboden M, Murphy KR, Rakhmilevich AL, Neal ZC, Xiang R, Reisfeld RA, et al.
593 The level of MHC class I expression on murine adenocarcinoma can change the
594 antitumor effector mechanism of immunocytokine therapy. Cancer Res.
595 2001;61(4):1500-7. PubMed PMID: WOS:000167255400047.
596 19. Morris ZS, Guy EI, Francis DM, Gressett MM, Werner LR, Carmichael LL, et al.
597 In Situ Tumor Vaccination by Combining Local Radiation and Tumor-Specific Antibody
598 or Immunocytokine Treatments. Cancer Res. 2016;76(13):3929-41. Epub 2016/05/20.
599 doi: 10.1158/0008-5472.CAN-15-2644. PubMed PMID: 27197149; PubMed Central
600 PMCID: PMCPMC4930687.
601 20. Neal ZC, Imboden M, Rakhmilevich AL, Kim KM, Hank JA, Surfus J, et al. NXS2
602 murine neuroblastomas express increased levels of MHC class I antigens upon
603 recurrence following NK-dependent immunotherapy. Cancer Immunol Immunother.
604 2004;53(1):41-52. Epub 20030918. doi: 10.1007/s00262-003-0435-2. PubMed PMID:
605 14504825; PubMed Central PMCID: PMCPMC11032988.
606 21. Albertini MR, Hank JA, Gadbaw B, Kostlevy J, Haldeman J, Schalch H, et al.
607 Phase II trial of hu14.18-IL2 for patients with metastatic melanoma. Cancer Immunol
608 Immunother. 2012;61(12):2261-71. Epub 2012/06/09. doi: 10.1007/s00262-012-1286-5.
609 PubMed PMID: 22678096; PubMed Central PMCID: PMCPMC3502633.
610 22. Albertini MR, Yang RK, Ranheim EA, Hank JA, Zuleger CL, Weber S, et al. Pilot
611 trial of the hu14.18-IL2 immunocytokine in patients with completely resectable recurrent
612 stage III or stage IV melanoma. Cancer Immunol Immunother. 2018;67(10):1647-58.
613 Epub 2018/08/04. doi: 10.1007/s00262-018-2223-z. PubMed PMID: 30073390; PubMed
614 Central PMCID: PMCPMC6168354.

615 23. King DM, Albertini MR, Schalch H, Hank JA, Gan J, Surfus J, et al. Phase I
616 clinical trial of the immunocytokine EMD 273063 in melanoma patients. J Clin Oncol.
617 2004;22(22):4463-73. Epub 2004/10/16. doi: 10.1200/JCO.2004.11.035. PubMed PMID:
618 15483010; PubMed Central PMCID: PMCPMC2367368.
619 24. Osenga KL, Hank JA, Albertini MR, Gan J, Sternberg AG, Eickhoff J, et al. A
620 phase I clinical trial of the hu14.18-IL2 (EMD 273063) as a treatment for children with
621 refractory or recurrent neuroblastoma and melanoma: a study of the Children's
622 Oncology Group. Clin Cancer Res. 2006;12(6):1750-9. Epub 2006/03/23. doi:
623 10.1158/1078-0432.CCR-05-2000. PubMed PMID: 16551859; PubMed Central PMCID:
624 PMCPMC2587020.
625 25. Shusterman S, London WB, Gillies SD, Hank JA, Voss SD, Seeger RC, et al.
626 Antitumor activity of hu14.18-IL2 in patients with relapsed/refractory neuroblastoma: a
627 Children's Oncology Group (COG) phase II study. J Clin Oncol. 2010;28(33):4969-75.
628 Epub 2010/10/06. doi: 10.1200/JCO.2009.27.8861. PubMed PMID: 20921469; PubMed
629 Central PMCID: PMCPMC3020698.
630 26. Hank JA, Gan J, Ryu H, Ostendorf A, Stauder MC, Sternberg A, et al.
631 Immunogenicity of the hu14.18-IL2 immunocytokine molecule in adults with melanoma
632 and children with neuroblastoma. Clin Cancer Res. 2009;15(18):5923-30. Epub
633 2009/09/10. doi: 10.1158/1078-0432.Ccr-08-2963. PubMed PMID: 19737959; PubMed
634 Central PMCID: PMCPMC2745522.
635 27. Navid F, Sondel PM, Barfield R, Shulkin BL, Kaufman RA, Allay JA, et al. Phase I
636 trial of a novel anti-GD2 monoclonal antibody, Hu14.18K322A, designed to decrease
637 toxicity in children with refractory or recurrent neuroblastoma. J Clin Oncol.

638 2014;32(14):1445-52. Epub 20140407. doi: 10.1200/jco.2013.50.4423. PubMed PMID:
639 24711551; PubMed Central PMCID: PMCPMC4017710.
640 28. Yu AL, Gilman AL, Ozkaynak MF, Naranjo A, Diccianni MB, Gan J, et al. Long-
641 Term Follow-up of a Phase III Study of ch14.18 (Dinutuximab) + Cytokine
642 Immunotherapy in Children with High-Risk Neuroblastoma: COG Study ANBL0032. Clin
643 Cancer Res. 2021;27(8):2179-89. Epub 20210127. doi: 10.1158/1078-0432.Ccr-20-
644 3909. PubMed PMID: 33504555; PubMed Central PMCID: PMCPMC8046731.
645 29. Schellekens H. Factors influencing the immunogenicity of therapeutic proteins.
646 Nephrol Dial Transplant. 2005;20 Suppl 6:vi3-9. doi: 10.1093/ndt/gfh1092. PubMed
647 PMID: 15958824.
648 30. Baniel CC, Sumiec EG, Hank JA, Bates AM, Erbe AK, Pieper AA, et al.
649 Intratumoral injection reduces toxicity and antibody-mediated neutralization of
650 immunocytokine in a mouse melanoma model. J Immunother Cancer. 2020;8(2). doi:
651 10.1136/jitc-2020-001262. PubMed PMID: 33115944; PubMed Central PMCID:
652 PMCPMC7594540.
653 31. Paoloni M, Mazcko C, Selting K, Lana S, Barber L, Phillips J, et al. Defining the
654 Pharmacodynamic Profile and Therapeutic Index of NHS-IL12 Immunocytokine in Dogs
655 with Malignant Melanoma. PLoS One. 2015;10(6):e0129954. Epub 20150619. doi:
656 10.1371/journal.pone.0129954. PubMed PMID: 26091536; PubMed Central PMCID:
657 PMCPMC4474860.
658 32. Parng C, Bolt M, Pittman DD, Caiazzo T, Dyleski L, Gorovits B, Webster R.
659 Induction and Impact of Anti-Drug Responses Elicited by a Human Recombinant

660 Coagulation Factor FXa(I16L) in Preclinical Species. Aaps j. 2019;21(3):52. Epub
661 20190411. doi: 10.1208/s12248-019-0324-z. PubMed PMID: 30976993.
662 33. Wong C, Muguiro DH, Lavergne S, Behling-Kelly E, Goggs R. Pharmacokinetics
663 of human recombinant C1-esterase inhibitor and development of anti-drug antibodies in
664 healthy dogs. Vet Immunol Immunopathol. 2018;203:66-72. Epub 20180823. doi:
665 10.1016/j.vetimm.2018.08.006. PubMed PMID: 30243377.
666 34. Jani M, Isaacs JD, Morgan AW, Wilson AG, Plant D, Hyrich KL, et al. Detection of
667 anti-drug antibodies using a bridging ELISA compared with radioimmunoassay in
668 adalimumab-treated rheumatoid arthritis patients with random drug levels.
669 Rheumatology (Oxford). 2016;55(11):2050-5. Epub 20160825. doi:
670 10.1093/rheumatology/kew299. PubMed PMID: 27565176; PubMed Central PMCID:
671 PMCPMC5088626.
672 35. Stubenrauch K, Wessels U, Birnboeck H, Ramirez F, Jahreis A, Schleypen J.
673 Subset analysis of patients experiencing clinical events of a potentially immunogenic
674 nature in the pivotal clinical trials of tocilizumab for rheumatoid arthritis: Evaluation of an
675 antidrug antibody ELISA using clinical adverse event-driven immunogenicity testing.
676 Clin Ther. 2010;32(9):1597-609. doi: 10.1016/j.clinthera.2010.07.021. PubMed PMID:
677 20974317.
678 36. Suh K, Kyei I, Hage DS. Approaches for the detection and analysis of antidrug
679 antibodies to biopharmaceuticals: A review. J Sep Sci. 2022;45(12):2077-92. Epub
680 20220310. doi: 10.1002/jssc.202200112. PubMed PMID: 35230731; PubMed Central
681 PMCID: PMCPMC9520450.

682 37. Vande Casteele N, Buurman DJ, Sturkenboom MG, Kleibeuker JH, Vermeire S,
683 Rispens T, et al. Detection of infliximab levels and anti-infliximab antibodies: a
684 comparison of three different assays. Aliment Pharmacol Ther. 2012;36(8):765-71. Epub
685 20120828. doi: 10.1111/apt.12030. PubMed PMID: 22928581.
686 38. Albertini MR, Zuleger CL, Ranheim EA, Shiyanbola O, Sondel PM, Morris ZS, et
687 al. Administration of intratumoral GD2-directed interleukin-2 immunocytokine and local
688 radiation therapy to activate immune rejection of spontaneous canine melanoma.
689 Melanoma Res. 2024;34(4):307-18. Epub 20240520. doi:
690 10.1097/CMR.0000000000000975. PubMed PMID: 38768442.
691 39. Magee K, Marsh IR, Turek MM, Grudzinski J, Aluicio-Sarduy E, Engle JW, et al.
692 Safety and feasibility of an in situ vaccination and immunomodulatory targeted
693 radionuclide combination immuno-radiotherapy approach in a comparative (companion
694 dog) setting. PLoS One. 2021;16(8):e0255798. Epub 20210812. doi:
695 10.1371/journal.pone.0255798. PubMed PMID: 34383787; PubMed Central PMCID:
696 PMCPMC8360580.
697 40. LeBlanc AK, Atherton M, Bentley RT, Boudreau CE, Burton JH, Curran KM, et al.
698 Veterinary Cooperative Oncology Group-Common Terminology Criteria for Adverse
699 Events (VCOG-CTCAE v2) following investigational therapy in dogs and cats. Vet Comp
700 Oncol. 2021;19(2):311-52. Epub 20210218. doi: 10.1111/vco.12677. PubMed PMID:
701 33427378; PubMed Central PMCID: PMCPMC8248125.
702 41. Hornbeck PV. Enzyme-Linked Immunosorbent Assays. Curr Protoc Immunol.
703 2015;110:2.1.-2.1.23. Epub 20150803. doi: 10.1002/0471142735.im0201s110. PubMed
704 PMID: 26237010.

705 42. R Core Team. R: A language and environment for statistical computing. The R
706 Foundation for Statistical Computing, Vienna, Austria. 2022.
707 43. Wickham H. ggplot2: Elegant Graphics for Data Analysis. Springer-Verlag New
708 York; 2016.
709 44. Wickham H. stringr: Simple, Consistent Wrappers for Common String
710 Operations. 2022.
711 45. Navid F, Santana VM, Barfield RC. Anti-GD2 antibody therapy for GD2-
712 expressing tumors. Curr Cancer Drug Targets. 2010;10(2):200-9. doi:
713 10.2174/156800910791054167. PubMed PMID: 20201786; PubMed Central PMCID:
714 PMCPMC2888262.
715 46. Butler JE, Ni L, Brown WR, Joshi KS, Chang J, Rosenberg B, Voss EW, Jr. The
716 immunochemistry of sandwich ELISAs--VI. Greater than 90% of monoclonal and 75% of
717 polyclonal anti-fluorescyl capture antibodies (CAbs) are denatured by passive
718 adsorption. Mol Immunol. 1993;30(13):1165-75. doi: 10.1016/0161-5890(93)90135-x.
719 PubMed PMID: 8413321.
720 47. Bergman D, Bäckström C, Hansson-Hamlin H, Larsson A, Holst BS. Pre-existing
721 canine anti-IgG antibodies: implications for immunotherapy, immunogenicity testing and
722 immunoassay analysis. Sci Rep. 2020;10(1):12696. Epub 20200729. doi:
723 10.1038/s41598-020-69618-3. PubMed PMID: 32728049; PubMed Central PMCID:
724 PMCPMC7391631.
725 48. Bergman D, Larsson A, Hansson-Hamlin H, Åhlén E, Holst BS. Characterization
726 of canine anti-mouse antibodies highlights that multiple strategies are needed to combat
727 immunoassay interference. Sci Rep. 2019;9(1):14521. Epub 20191010. doi:

728 10.1038/s41598-019-51228-3. PubMed PMID: 31601945; PubMed Central PMCID:
729 PMCPMC6787031.
730 49. Goldberg JL, Navid F, Hank JA, Erbe AK, Santana V, Gan J, et al. Pre-existing
731 antitherapeutic antibodies against the Fc region of the hu14.18K322A mAb are
732 associated with outcome in patients with relapsed neuroblastoma. J Immunother
733 Cancer. 2020;8(1). doi: 10.1136/jitc-2020-000590. PubMed PMID: 32169872; PubMed
734 Central PMCID: PMCPMC7069273.
735 50. Harding FA, Stickler MM, Razo J, DuBridge RB. The immunogenicity of
736 humanized and fully human antibodies: residual immunogenicity resides in the CDR
737 regions. MAbs. 2010;2(3):256-65. Epub 20100501. doi: 10.4161/mabs.2.3.11641.
738 PubMed PMID: 20400861; PubMed Central PMCID: PMCPMC2881252.
739 51. Baniel CC, Heinze CM, Hoefges A, Sumiec EG, Hank JA, Carlson PM, et al. In
740 situ Vaccine Plus Checkpoint Blockade Induces Memory Humoral Response. Front
741 Immunol. 2020;11:1610. Epub 20200724. doi: 10.3389/fimmu.2020.01610. PubMed
742 PMID: 32849544; PubMed Central PMCID: PMCPMC7396490.
743 52. Nabrinsky E, Macklis J, Bitran J. A Review of the Abscopal Effect in the Era of
744 Immunotherapy. Cureus. 2022;14(9):e29620. Epub 20220926. doi:
745 10.7759/cureus.29620. PubMed PMID: 36321062; PubMed Central PMCID:
746 PMCPMC9604762.
747 53. Brichory FM, Misek DE, Yim AM, Krause MC, Giordano TJ, Beer DG, Hanash
748 SM. An immune response manifested by the common occurrence of annexins I and II
749 autoantibodies and high circulating levels of IL-6 in lung cancer. Proc Natl Acad Sci U S

750 A. 2001;98(17):9824-9. doi: 10.1073/pnas.171320598. PubMed PMID: 11504947;
751 PubMed Central PMCID: PMCPMC55537.
752 54. Reuschenbach M, von Knebel Doeberitz M, Wentzensen N. A systematic review
753 of humoral immune responses against tumor antigens. Cancer Immunol Immunother.
754 2009;58(10):1535-44. Epub 20090628. doi: 10.1007/s00262-009-0733-4. PubMed
755 PMID: 19562338; PubMed Central PMCID: PMCPMC2782676.
756 55. Fischer E, Kobold S, Kleber S, Kubuschok B, Braziulis E, Knuth A, et al. Cryptic
757 epitopes induce high-titer humoral immune response in patients with cancer. J Immunol.
758 2010;185(5):3095-102. Epub 20100726. doi: 10.4049/jimmunol.0902166. PubMed
759 PMID: 20660712.
760 56. German AJ, Hall EJ, Day MJ. Measurement of IgG, IgM and IgA concentrations
761 in canine serum, saliva, tears and bile. Vet Immunol Immunopathol. 1998;64(2):107-21.
762 doi: 10.1016/s0165-2427(98)00132-9. PubMed PMID: 9661261.
763

764 # Supporting information

765 **S1 Fig. Binding inhibition assay controls.** PE-conjugated anti-GD2 antibody 14G2a
766 was mixed with either (A) 20 μl (open histogram with solid line) or (B) 2.5 μl (open
767 histogram with solid line) healthy canine donor sera before staining M21 cells. M21
768 stained with 14G2a-PE mixed with 20 μl or 2.5 μl PBS as a no-serum control is
769 represented as a gray histogram in both (A) and (B). Data are representative of
770 triplicates. Values represent % binding inhibition compared to no-serum control.
771

772 **S2 Fig. Serum from dogs treated with hu14.18-IL2 shows varied level of inhibition**
773 **of 14G2a binding to target GD2.** Prior to staining M21 cells, PE-conjugated anti-GD2
774 antibody 14G2a was mixed with baseline/pre-treatment sera or post-treatment sera
775 from different timepoints from (A) K914 or (B) K915. Baseline/pre-treatment data are
776 represented as gray histograms; post-treatment data are represented as open
777 histograms with solid lines. Data are representative of triplicates. Values represent %
778 binding inhibition compared to baseline/pre-treatment control.

Data availability statement

All relevant data are within the manuscript and its Supporting Information files.

Funding

Supported by Merit Review Award I01 BX003916 from the Biomedical Laboratory Research and Development Service of the United States (U.S.) Department of Veterans Affairs (MRA), the University of Wisconsin Carbone Cancer Center (UWCCC) Cancer Pharmacology Laboratory and Flow Cytometry Laboratory (grant 1S10OD018202-01) supported by P30 CA014520 (NIH/HHS), the Barbara A. Suran Comparative Research Endowment (DMV), melanoma research gifts to the UWCCC (Tim Eagle Memorial (MRA), gift from Jill and Bob Freiermuth (MRA)), and use of facilities at the William S. Middleton Memorial Veterans Hospital, Madison, WI. The contents do not represent the views of the U.S. Department of Veterans Affairs or the United States Government. Anyxis Immuno-Oncology Gmbh is the current license holder for hu14.18-IL2 and provided hu14.18-IL2 for this program of research. The funders had no role in study design, data collection and analysis, decision to publish, or preparation of the manuscript.

Competing interests

None

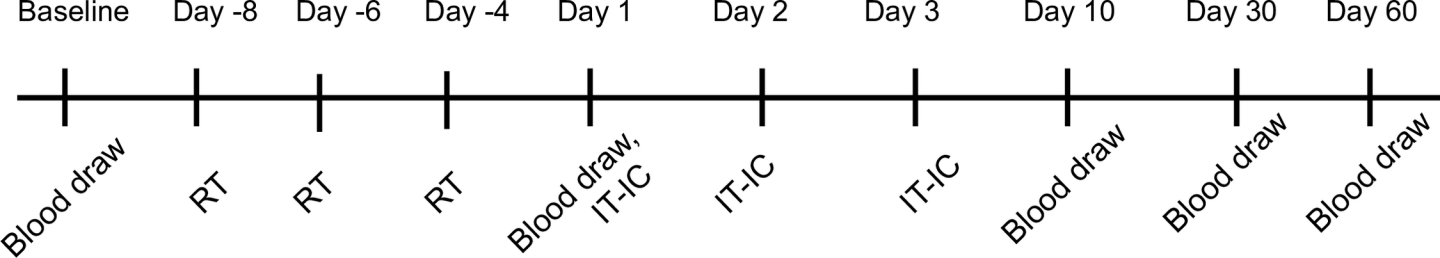
Baseline
Day -8
Day -6
Day -4
Day 1
Day 2
Day 3
Day 10
Day 30
Day 60
Blood draw
RT
RT
RT
Blood draw, IT-IC
IT-IC
IT-IC
Blood draw
Blood draw
Blood draw

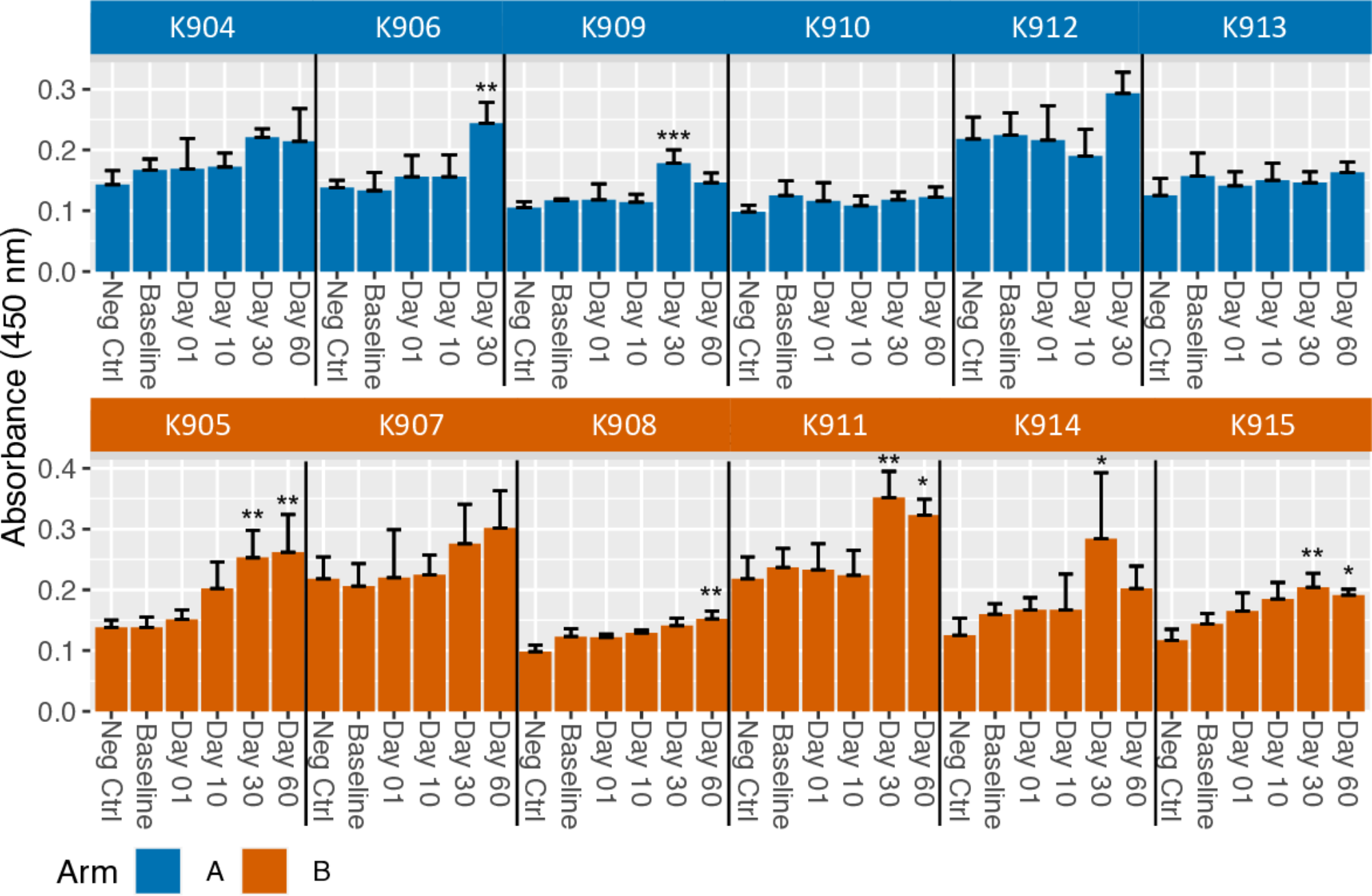
K904
K906
K909
K910
K912
K913
K905
K907
K908
K911
K914
K915
Absorbance (450 nm)
0.0
0.1
0.2
0.3
0.4
Neg Ctrl
Baseline
Day 01
Day 10
Day 30
Day 60
**
***
*
Arm
A
B

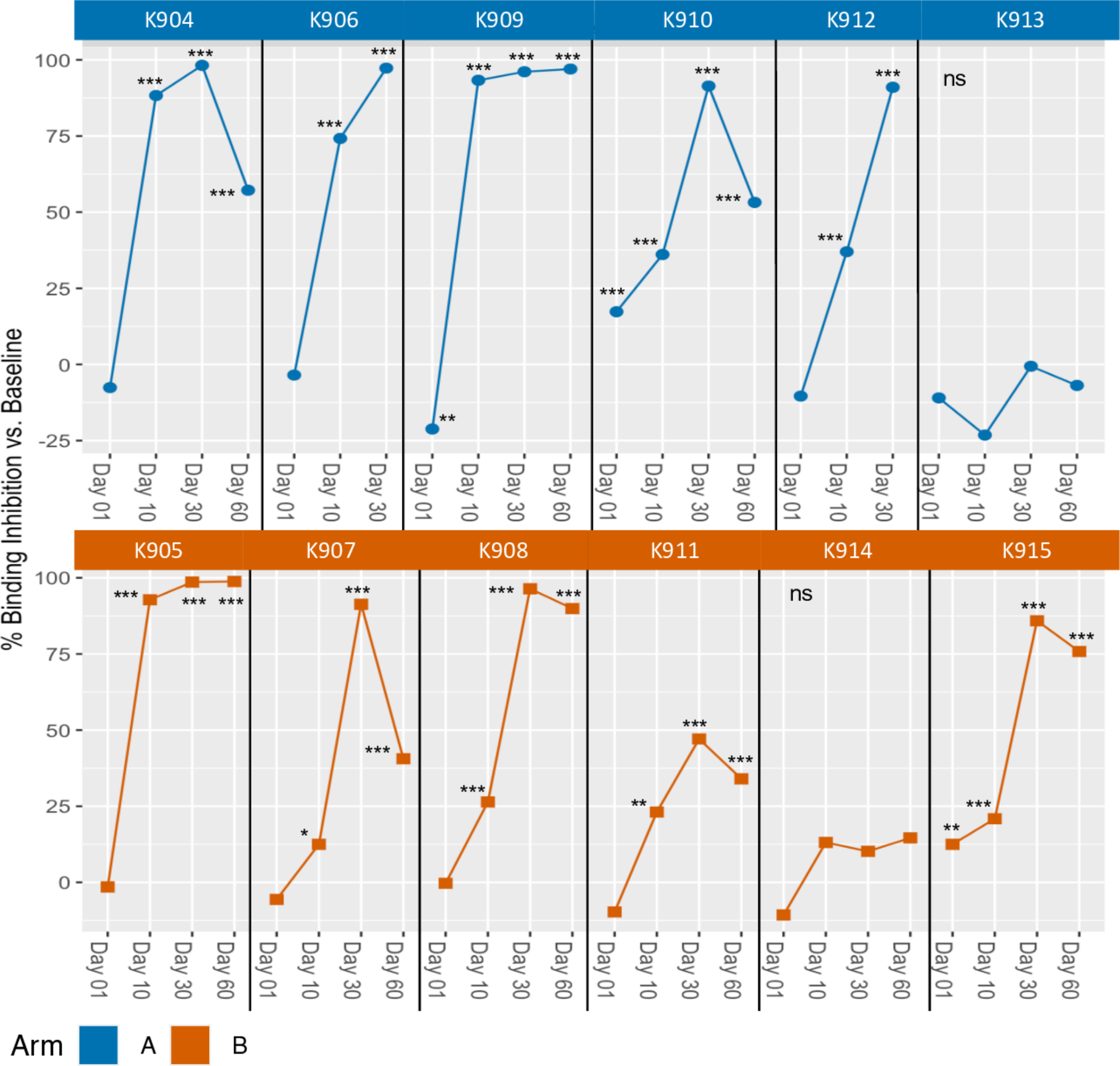
K904
K906
K909
K910
K912
K913
K905
K907
K908
K911
K914
K915
% Binding Inhibition vs. Baseline
100
75
50
25
0
-25
Day 01
Day 10
Day 30
Day 60
ns
Arm
A
B

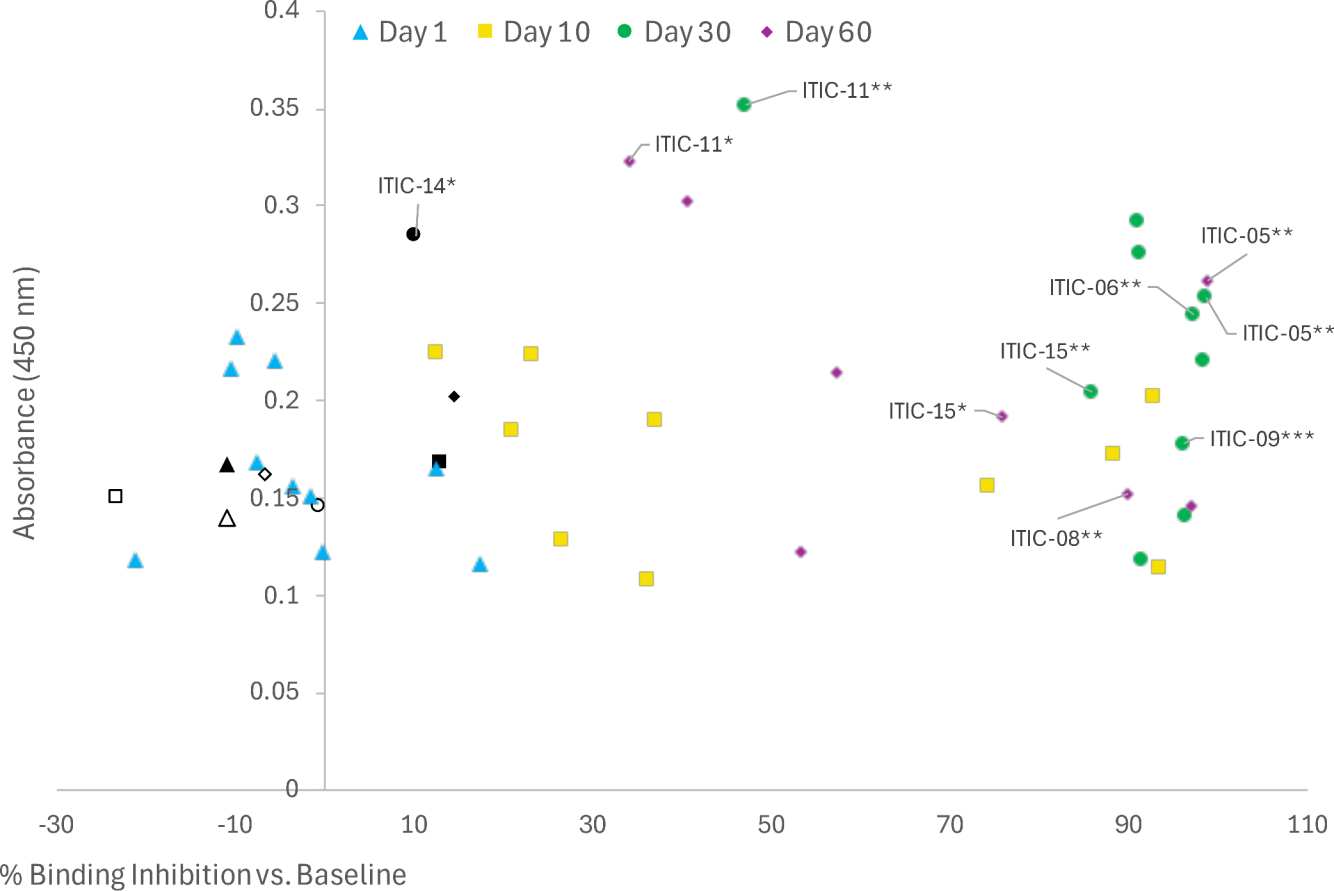
Day 1
Day 10
Day 30
Day 60
ITIC-11**
ITIC-11*
ITIC-14*
ITIC-05**
ITIC-06**
ITIC-05**
ITIC-15**
ITIC-15*
ITIC-09***
ITIC-08**
Absorbance (450 nm)
0.4
0.35
0.3
0.25
0.2
0.15
0.1
0.05
0
-30
-10
10
30
50
70
90
110
% Binding Inhibition vs. Baseline

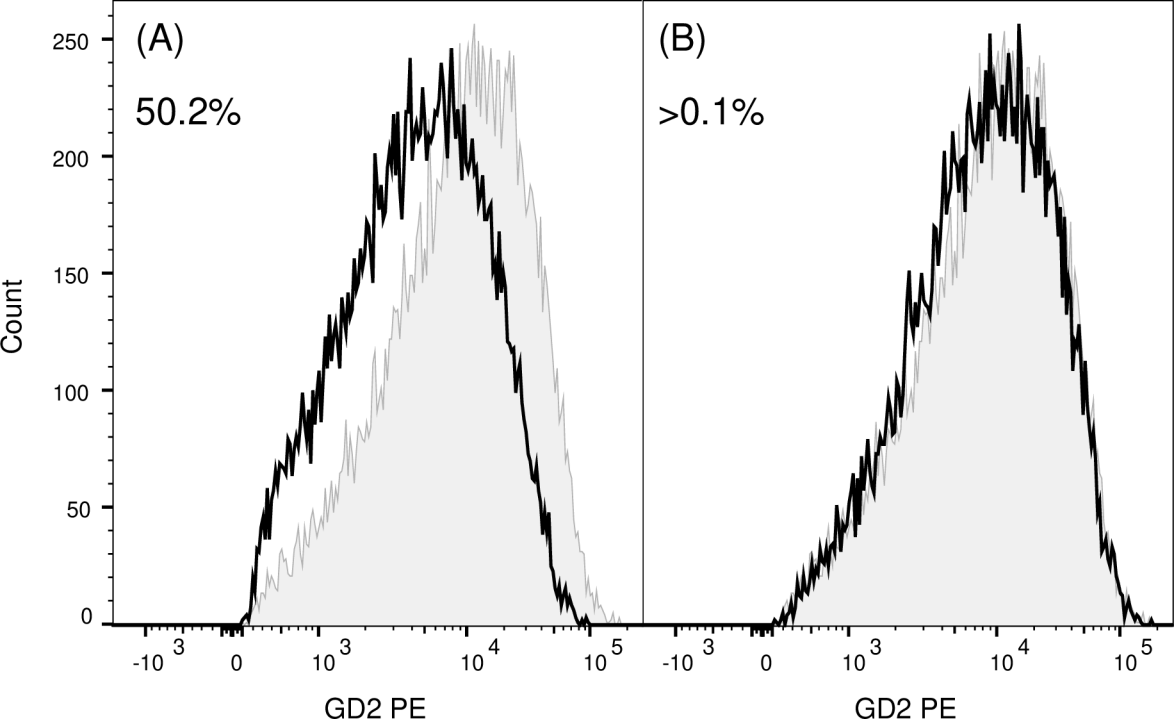
(A)
50.2%
(B)
>0.1%
Count
250
200
150
100
50
0
-10 3
0
10 3
10 4
10 5
GD2 PE

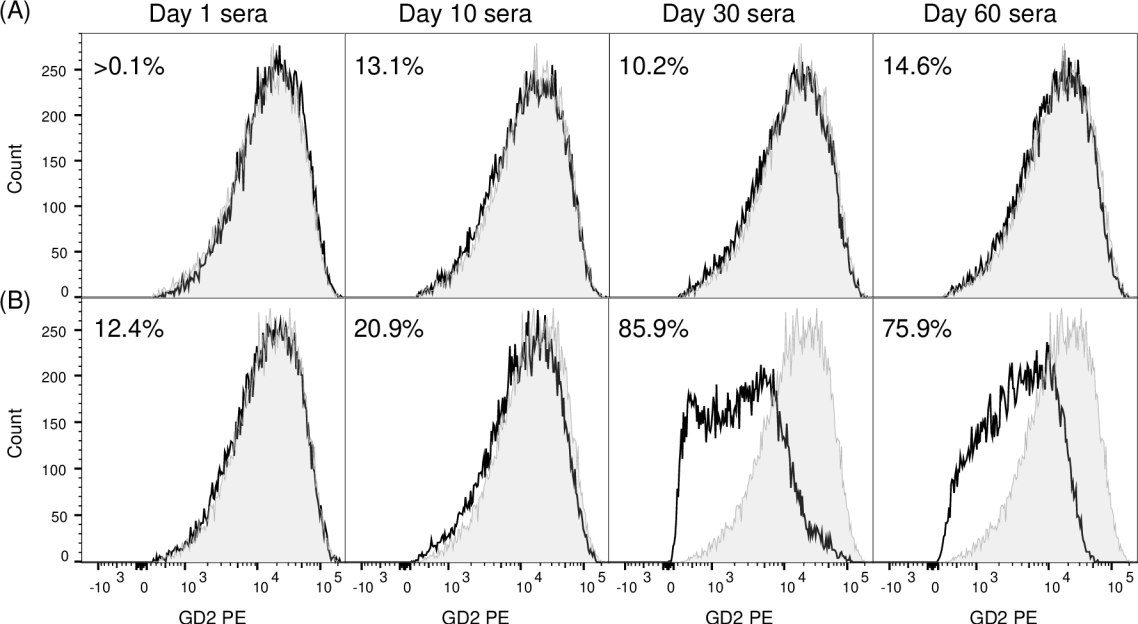
(A)
Day 1 sera
Day 10 sera
Day 30 sera
Day 60 sera
>0.1%
13.1%
10.2%
14.6%
(B)
12.4%
20.9%
85.9%
75.9%
Count
250
200
150
100
50
0
-10 3
0
10 3
10 4
10 5
GD2 PE